X-ray computed tomography tracking of the calcium chloride hexahydrate crystallisation process

Journal of Physics: Conference Series **2766** (2024) 012082 doi:10.1088/1742-6596/2766/1/012082

X-ray computed tomography tracking of the calcium chloride hexahydrate crystallisation process

Dario Guarda[1], Jorge Martinez-Garcia[2], Benjamin Fenk[2], Damian Gwerder[2], Anastasia Stamatiou[2], Jörg Worlitschek[2], Simone Mancin[1] and Philipp Schuetz[2]

[1]Department of Management and Engineering, University of Padova, Str.lla S.Nicola 3, Vicenza, 36100, Italy
[2]Competence Centre for Thermal Energy Storage, Lucerne University of Applied Sciences and Arts, Technikumstrasse 21, Horw, 6048, Switzerland

Email: dario.guarda@unipd.it

Abstract. The research conducted on phase change materials (PCMs) for latent thermal energy storages (LTESs) is continuously growing in terms of publications, highlighting the importance of this topic. In fact, PCMs present many advantages that could help the energy transition and reduce CO_2 emissions, by enhancing the performance of existing systems and better exploiting renewable energy. Therefore, it is of crucial interest to develop new and reliable methods to control LTES. Differently from sensible thermal energy storages, in LTESs the stored thermal energy is not proportional to the temperature. To really have an insight into the level of charge of these storages, it is important to know the liquid fraction, i.e., the amount of the liquid phase with respect to the whole amount of PCM. X-ray computed tomography (XCT) is a technology that allows to non-intrusively "look inside" the materials. In the current study, it was used to analyse the calcium chloride hexahydrate crystallization. This transient process of calcium chloride hexahydrate was tracked with a sequence of XCT scans, one every 6 minutes, resulting in 3D image stacks that were processed to obtain the volumetric liquid fraction evolution over time. Repeatability tests were run to evaluate the reliability of the XCT technique and the volumetric liquid fraction data was used to validate a numerical model developed within ANSYS Fluent framework. XCT offers great opportunities to study the heat and mass transfer mechanisms underlying the main issues of phase change materials, like, for example, supercooling and salt hydrate segregation.

1. Introduction

Latent thermal energy storages (LTESs) are of paramount importance towards the energy transition, and the study of the materials needed to implement this technology is at its peak. Phase change materials (PCMs), in fact, still face unsolved challenges that have to be addressed to reduce cost, enhance efficiency and prolong the operational life of LTESs. For this reason, new methodologies to experimentally assess the behaviour of PCMs need to be considered. In the present work, a recent approach to measure liquid fraction of PCM is assessed and used to study further study calcium chloride hexahydrate. The liquid fraction is defined as the share of liquid PCM in a system that is melting or solidifying. Liquid fraction was previously obtained from video cameras, temperature sensors, or a combination of both [1,2]. Unfortunately, these technologies only resulted in 2D (video cameras) or local (temperature sensors) information. A fully detailed volumetric map of the liquid fraction inside a PCM system cannot be extracted with these technologies. To overcome this limitation, X-ray computed tomography (XCT) has been recently considered to study PCMs [3–7]. XCT could give further insight

for materials like salt hydrates, which still present different issues, such as segregation. Dannemand et al. [8] and Kohler et al. [9] were the firsts to study salt hydrates with the XCT technique for LTES applications.
Dannemand et al. [8] analysed sodium acetate trihydrate (SAT): the authors found that the density of the solid phase depends on the degree of supercooling and they observed a discrepancy between the density reported in literature for solid SAT and their measurements.
Kohler et al. [9] studied another salt hydrate: magnesium chloride hexahydrate. The authors were able to analyse a tube-in-tube heat exchanger containing the salt hydrate and they did not observe any supercooling or phase separation phenomena. One of their main concluding remarks was related to the volume shrinkage, which could lead to some issues if not properly handled. They observed that solidification started both from the heat-exchanger inner tube and also from its outer wall leaving a cavity in between these zones.
Martinez-Garcia et al. [3,5,6] and Guarda et al. [4,7] were the firsts to propose a systematic approach to measure volumetric liquid fraction via XCT aiming at the study of non-metallic PCMs. They studied ice-water, eicosane, and calcium chloride hexahydrate, the latter being object of the current analysis. In this work, in fact, an in-depth XCT analysis of calcium chloride hexahydrate is presented, trying to assess the repeatability of the systematic volumetric liquid fraction measurement methodology.

2. Experimental and numerical setup

The PCM analysed is calcium chloride hexahydrate, $CaCl_2 \cdot 6H_2O$, (CAS number: 7774-34-7). This salt hydrate exhibits a melting point around 29.4°C [10].

2.1. Experiments

Three dynamic XCT measurements were performed on three $CaCl_2 \cdot 6H_2O$ samples that were prepared following the same procedure: the material was weighted (62.0±0.1 g), put inside a cylindrical glass vial container (30 mm diameter) and melted in an oven at 50°C before being placed inside the XCT chamber to be solidified at ambient temperature (20°C) while the scans were acquired. In figure 1, the experimental setup of the XCT is shown. X-rays are generated in the source and directed towards the detector, passing through the sample, which stands on a plate that rotates while acquiring the scans.
The XCT machine is a Diondo D2 system from Diondo, Hattingen, Germany. The measurements were conducted with the X-ray source XWT-225 TCHE+. The X-ray tube was set to 160 kV with a tube current of 156 µA (i.e., power of 24.96 W) in the high power focus setting. The filter used is a 1.0 mm thick layer of aluminium [3]. A 4343 XCT detector from Varex, Salt Lake City, U.S.A, having pixel size of 150 µm, was used. The amplification capacity was set to 8 pF, without pixel binning and 4 frames were binned. An integration time of 170 ms was used to acquire 400 projections, resulting in a scan time of 4 min and 53 s per time step. The reconstruction was performed with the Cera software package from Siemens Healthineers, Erlangen, Germany. This software is based on the Feldkamp-Davis-Kress algorithm [11]. The reconstructed images, with cubic voxels of 103 µm edge length, have dimensions of 400 x 400 x 1516 voxels. Beam hardening correction 4 of the Cera software was applied. All the stacks were reconstructed with the same fixed scale for comparison purpose.
The software used to visualise and postprocess the 3D image stacks of the dynamic measurement are ImageJ-2.0, GeoDict®2021 which supported the algorithms developed in-house via Python 3.7. The algorithm to compute volumetric liquid fractions is based on Otsu thresholding method [12]. Further details on the algorithm can be found in Martinez-Garcia et al. [3].

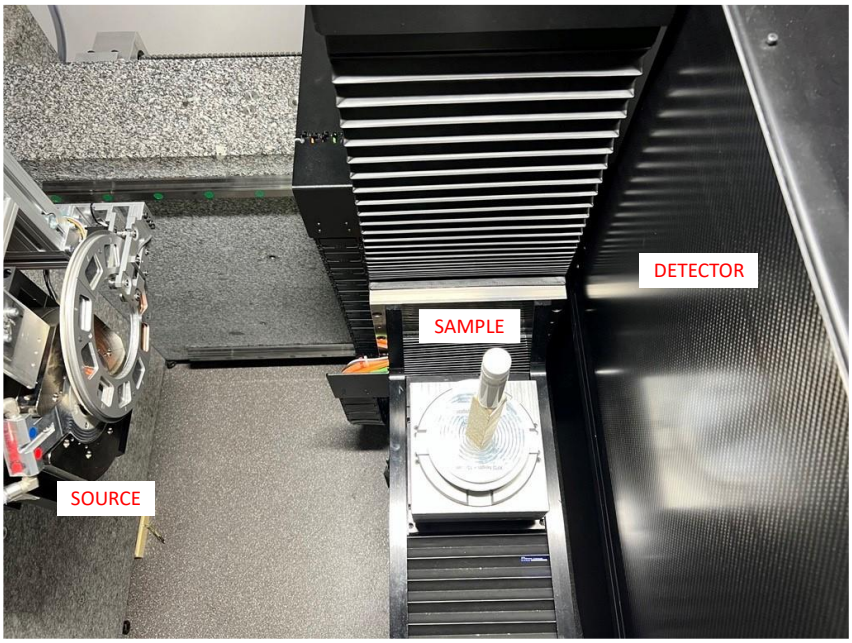

Figure 1. View on the X-ray computed tomography setup in the cabinet.

2.2. Simulations

The computational fluid dynamics (CFD) software used for the simulations was Ansys Fluent 18.2. The domain is reported in figure 2. The axial symmetric domain is initialized at 50°C, with the bottom being adiabatic. A natural convection boundary condition is assigned to the other walls (10 W m^{-2} K^{-1} heat transfer coefficient and 20°C free stream temperature as in [4,7]).

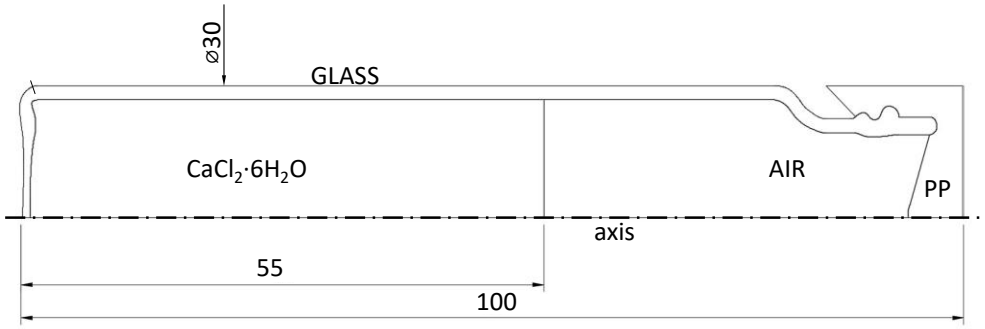

Figure 2. Domain of the CFD simulations with boundary and initial conditions. Values are given in mm.

The current CFD model is based on the enthalpy-porosity method [13]. Ansys Fluent solves the equations representing the conservation of mass, momentum, and energy (1-3). ρ is the density (kg m^{-3}), v the velocity (m s^{-1}), p the pressure (Pa), τ the stress tensor (Pa), g the gravitational acceleration (m s^{-2}), A_{mush} the mushy zone constant (kg m^{-3} s^{-1}), h and H the enthalpy (J kg^{-1}), k the thermal conductivity (W m^{-1} K^{-1}), T the temperature (K) and t is time (s). The liquid fraction (γ) is defined in (4), where $T_{solidus}$ and $T_{liquidus}$ are the delimiting temperatures of the melting range. The mushy zone constant A_{mush} was set to its default value of 10^5 kg m^{-3} s^{-1}.

The dynamics of the system was based on the following model equations:

$$\frac{\partial \rho}{\partial t} + \nabla \cdot (\rho \vec{v}) = 0 \quad (1)$$

$$\frac{\partial}{\partial t}(\rho\vec{v}) + \nabla\cdot(\rho\vec{v}\vec{v}) = -\nabla \mathrm{p} + \nabla\cdot(\bar{\bar{\tau}}) + \rho\vec{g} + \frac{(1-\gamma)^2}{(\gamma^3+0.001)}A_{mush}\vec{v} \quad (2)$$

$$\frac{\partial}{\partial t}(\rho H) + \nabla\cdot(\rho\vec{v}H) = \nabla\cdot(k\nabla \mathrm{T}) \quad (3)$$

$$\gamma = \begin{cases} 0 & if\ T < T_S \\ \frac{T-T_{solidus}}{T_{liquidus}-T_{solidus}} & if\ T_S < T < T_L \\ 1 & if\ T > T_L \end{cases} \quad (4)$$

Equation (2) is the conservation of momentum: the left-hand side of the equations represents the total derivative of velocity, while on the right-hand side, pressure, viscous, and gravitational effects are considered. The last term is a source term of the enthalpy-porosity method, accounting for higher pressure drops as the liquid fraction increases.
Density was considered constant (equal to ρ_0) in all the equations except for the momentum conservation, where the Boussinesq approximation was used (5). β is the thermal expansion coefficient (K^{-1}).

$$\rho = \rho_0(1 - \beta\,\Delta T) \quad (5)$$

The energy equation is written in terms of enthalpy: H is the sum between sensible and latent enthalpy (6). H_{ref} is the reference enthalpy (J kg^{-1}) corresponding to temperature T_{ref} (K), c_p is the specific heat (J kg^{-1} K^{-1}) and L is the latent heat of fusion (J kg^{-1}).

$$H = \left(h_{ref} + \int_{T_{ref}}^{T} c_p dT\right) + (\gamma L) \quad (6)$$

The materials associated with the different zones of the domain are: $CaCl_2{\cdot}6H_2O$, air, glass, polypropylene (PP). The properties of $CaCl_2{\cdot}6H_2O$ are reported in table 1, [14]. The air inside the sample is assumed not to be moving significantly, thus it was modelled as a solid (density of 1.139 kg m^{-3}, specific heat of 1006 J kg^{-1} K^{-1} and thermal conductivity of 0.027 W m^{-1} K^{-1} [15]). The borosilicate glass density is 2230 kg m^{-3}, with a specific heat of 800 J kg^{-1} K^{-1} and a thermal conductivity of 1.2 W m^{-1} K^{-1} [16]), and the cap material is polypropylene (PP, density of 900 kg m^{-3}, specific heat of 1700 J kg^{-1} K^{-1} and thermal conductivity of 0.2 W m^{-1} K^{-1} [17]).

Table 1. Calcium chloride hexahydrate properties used in the CFD simulations.

$CaCl_2{\cdot}6H_2O$ Property (unit of measure)	Value
Density, solid/liquid (kg m^{-3})	1802/1562
Specific heat, solid/liquid (J kg^{-1} K^{-1})	1429/2100
Thermal conductivity, solid/liquid (W m^{-1} K^{-1})	1.088/0.54
Dynamic viscosity (Pa s)	0.0118
Thermal expansion coefficient (K^{-1})	0.003305
Latent enthalpy (kJ kg^{-1})	190.8
Solidus/liquidus temperature (°C)	28.5/30.5

A time step size of 0.1 s and a mesh size of 7876 elements were used, similarly to what suggested by Guarda et al. [7]. For pressure-velocity coupling, the SIMPLE algorithm was used, as well as PRESTO! for pressure spatial discretization. Further details on the model can be found in [4,7].

3. Results

In figure 3, the evolution of the volumetric liquid fraction over time is reported for the three repeatability measurements. A measurement uncertainty of ±0.08 liquid fraction was considered. The uncertainty was obtained by changing the solid-liquid threshold in the liquid fraction calculation algorithm [3] of a factor equal to the ratio between standard deviation and mean of the grey levels of the PCM. Considering this uncertainty, it is possible to affirm that the experimental procedure is repeatable. Observing the three experimental curves, after the onset of the crystallization, the volumetric liquid fraction trend is almost linear. A liquid phase is present at the end of the process, and this effect is probably due to the kinetics of the solidification: for this reason, the experimental liquid fractions did not reach 0 (fully solidified PCM).

The numerical liquid fraction (red curve) is also linear over time during the crystallisation. The model does not account for the residual liquid phase, thus, the red curve reaches 0 after about 320 min. According to the measurement uncertainty, it is possible to affirm that the numerical and experimental liquid fractions agree remarkably: the mean absolute deviation between experimental and numerical liquid fraction curves is 0.051. Figure 3 also shows three cross sections of the PCM solidification process. These grey value XCT images show solid (lighter) and liquid (darker) phases while the black zone is the air.

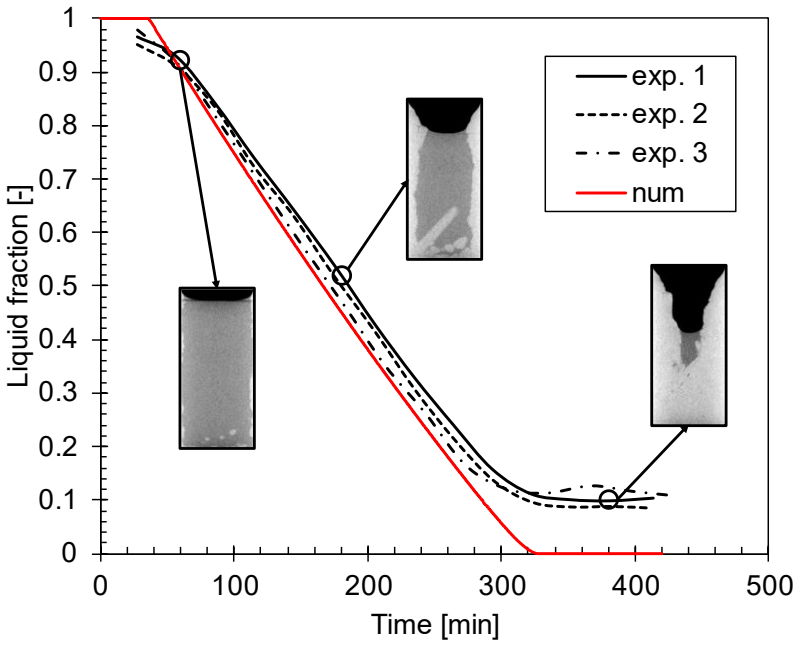

Figure 3. Experimental and numerical liquid fraction comparison.

4. Conclusions

In the present work, the crystallisation of calcium chloride hexahydrate is studied by means of dynamic X-ray computed tomography. Different XCT scans are acquired while the phase change process is progressing. An assessment on the repeatability of the experimental procedure is proposed. A numerical CFD model is considered to simulate the process.

The experiments are found to be repeatable, and the numerical model can reproduce the experimental data within the measurement error. Only at the end of the crystallisation, where the remaining liquid

solution is not accounted in the model, the numerical and experimental liquid fractions are significantly different one from the other. This experimental study provides evidence that the numerical models are describing the actual process sufficiently and may be used in the future for the optimisation of LTES systems.

5. References

[1] Mancin S, Calati M and Guarda D 2022 Experimental Techniques and Challenges in Evaluating the Performance of PCMs *Solid–Liquid Thermal Energy Storage* ed M Mobedi, K Hooman and W-Q Tao (CRC Press)
[2] Seddegh S, Wang X, Joybari M M and Haghighat F 2017 Investigation of the effect of geometric and operating parameters on thermal behavior of vertical shell-and-tube latent heat energy storage systems *Energy* **137** 69–82
[3] Martinez-Garcia J, Gwerder D, Wahli F, Guarda D, Fenk B, Stamatiou A, Worlitschek J and Schuetz P 2023 Volumetric quantification of melting and solidification of phase change materials by in-situ X-ray computed tomography *J Energy Storage* **61** 1-9
[4] Guarda D, Wahli F, Gwerder D, Martinez-Garcia J, Stamatiou A, Worlitschek J, Mancin S and Schuetz P 2022 Phase Change Material numerical simulation: enthalpy-porosity model validation against liquid fraction data from an X-ray computed tomography measurement/system *Nondestructive Testing and Evaluation* **37** 508-518
[5] Martinez-Garcia J, Gwerder D, Wahli F, Guarda D, Stamatiou A, Fischer L J, Worlitschek J and Schütz P 2022 Fully volumetric tracking of melting fronts in phase change materials with computed tomography *Proc. of the 11th Conf. on Industrial Computed Tomography (iCT), 8-11 Feb* vol 27 (Wels, Austria)
[6] Martinez-Garcia J, Gwerder D, Guarda D, Fenk B, Stamatiou A, Wortlitscheck J and Schuetz P 2023 Study of the solidification behaviour of phase change materials by in-situ X-ray computed tomography *Research and Review Journal of Nondestructive Testing (ReJNDDT)* **1**
[7] Guarda D, Martinez-Garcia J, Fenk B, Schiffmann D, Gwerder D, Stamatiou A, Worlitschek J, Mancin S and Schuetz P 2023 New liquid fraction measurement methodology for phase change material analysis based on X-ray computed tomography *Int J Therm Sci* **194** 1-10
[8] Dannemand M, Delgado M, Lazaro A, Penalosa C, Gundlach C, Trinderup C, Johansen J B, Moser C, Schranzhofer H and Furbo S 2018 Porosity and density measurements of sodium acetate trihydrate for thermal energy storage *Appl Therm Eng* **131** 707–14
[9] Kohler T, Kögl T and Müller K 2018 Study of the Crystallization and Melting Behavior of a Latent Heat Storage by Computed Tomography *Chem Ing Tech* **90** 366–71
[10] Hale D V., Hoover M J and O'Neill M J 1971 *Phase Change Materials Handbook* (Nasa Contractor Report Nasa Cr-51363)
[11] Feldkamp L A, Davis L C and Kress J W 1984 *Practical cone-beam algorithm* vol 1
[12] Otsu N 1979 A Threshold Selection Method from Gray-Level Histograms *IEEE Trans Syst Man Cybern* **SMC-9** 62–6
[13] Voller V R, Cross M and Markatos N C 1987 An Enthalpy Method for Convection/Diffusion Phase Change *Int J Numer Methods Eng* **24** 271–84
[14] Lane G A 1986 *Solar Heat Storage: Latent Heat Material: Volume II: Technology* (CRC Press)
[15] Engineering ToolBox 2003 Air - Thermophysical Properties
[16] Anon Scientific Glass Laboratories Ltd
[17] Material Properties Polypropylene – Density – Strength – Melting Point – Thermal Conductivity